

Short Communication

## Development of an Electrochemical Sensor for Catecholamine Detection via a Layer-by-layer Fabrication Method

Ruzheng Han<sup>1#</sup>, Jun Ma<sup>2#\*</sup> and Limin He<sup>2</sup>

<sup>1</sup> Department of Neurosurgery, Weihaiwei People's Hospital, Weihai 264200, P.R. China

<sup>2</sup> Department of Neurosurgery, 404 Central Hospital of The People's Liberation Army, Weihai, 264200, P.R. China

<sup>#</sup>These authors contributed equally to this work.

\* E-mail: [junma.826@foxmail.com](mailto:junma.826@foxmail.com)

Received: 18 July 2017 / Accepted: 5 September 2017 / Published: 12 October 2017

---

In this work, the Cu/MnO<sub>2</sub>/MWCNTs (MWCNTs) nanocomposite modified glass carbon electrode (GCE) was applied to the preparation of a novel sensor of catecholamine (CA) using an electrochemical strategy. Amperometry was used to investigate the electrocatalytic activity of this sensor in CA oxidation. It was found that the current response had a linear relationship with the concentration of glucose (0.65–2000 μM), and the correlation coefficient was 0.99. Meanwhile, the limit of detection (LOD) was calculated as 0.14 μM (S/N=3), and the response time was 3 s.

---

**Keywords:** Neurotransmitter Catecholamine; Layer-by-layer; Electrochemical determination; Cerebrovascular diseases

### 1. INTRODUCTION

Cardiovascular and cerebrovascular diseases are common diseases that affect human health. According to previous literature, severe temperature changes significantly correlate with the onset of cardio-cerebrovascular diseases. Studies have been conducted on the effects of cold air on patients with cerebrovascular and cardiovascular diseases [1-4]. The exposure to cold air causes an instant increase in human and animal blood sugar, as shown in epidemiologic and animal experimental reports. Therefore, cold air plays a vital role in cardio-cerebrovascular diseases [5-10]. Fluctuation in blood sugar is under the regulation of more than one hormone (such as catecholamines (CA), which could cause sharp increases or decreases in blood pressure) [11-15]. Therefore, CA is a main factor in the occurrence, development, and outcome of cardio-cerebrovascular diseases. Unfortunately, the effects of temperature change on the level of CA, and consequently on the cardio-cerebrovascular

diseases, have been rarely reported. To study the occurrence, development, and outcomes of cardiovascular diseases, the present work simulated the effects of cold air on human and experimental animal CA levels. Therefore, it is necessary to develop a sensitive strategy for the detection of CA.

In the past few years, the preparation of voltammetric sensors for the detection of catecholamine neurotransmitters (CNs) has gained substantial attention. These sensors are significant in different physical, pharmacological and biological processes [16]. In recent years, a new generation of decorated electrodes (such as nanoparticles, conductive polymers, monolayers, etc.) are urgently being developed to solve the issues present in traditional electrodes. Recently, substantial attention has been paid to metal oxide ( $\text{Cu}_x\text{O}$  [17],  $\text{MnO}_2$  [18],  $\text{Co}_3\text{O}_4$  [19], etc.) and metal hydroxide (such as  $\text{Cu}(\text{OH})_2$  [20]) – based non-enzymatic sensors, which show many advantages, including low cost, desirable stability, low LOD, high sensitivity, and rapid response. Their disadvantages include undesirable selectivity to other carbohydrates (sucrose, fructose, etc.). Electrochemical sensors involving nanocomposites composed of metal and metal oxide were prepared to settle this issue. The synergy effect brought by the integration of metal and metal oxide may enhance the performance of electrochemical sensors. Increasing attention has been paid to the metal oxides, including  $\text{MnO}_2$ ,  $\text{ZrO}_2$ ,  $\text{ZnO}$ ,  $\text{CuO}_2$ , and  $\text{SiO}_2$ , particularly to their flexible preparation, low cost, distinct chemical stability, and large specific surface area [21-24].

Recently, MWCNTs have gained extensive attention from scientific fields worldwide, both experimentally and theoretically. MWCNTs could promote the sensor behaviours because of their distinct electrical conductivity and large specific surface area; they are regarded as excellent for the sensing field in the case of electrochemistry [25-27]. Furthermore, nanoparticles modified with MWCNTs have recently become more popular. The composites of MWCNTs with other functional nanomaterials such as metal nanoparticles and polymers have received substantial study in the past few years [28-30]. Based on previous studies, the hybridization of these materials and MWCNTs could promote the functional features of each constituent element, and certain novel features could be obtained through cooperative interaction [31-34].

This report investigated the electrochemistry of CA in the presence of the  $\text{Cu}/\text{MnO}_2/\text{MWCNTs}$  nanocomposites. Herein a desirable electrochemical sensing platform was successfully developed. In addition, MWCNTs could be further applied to the fabrication of electrochemical sensors.

## 2. EXPERIMENTS

### 2.1. Chemicals and instruments

Multiwall carbon nanotubes (MWCNTs, high purity of >95%) were commercially available from Chengdu Organic Chemicals Co. Ltd. of the Chinese Academy of Science. Hydrazine solution (50%, wt/wt) was commercially available from Tianjin Yaohua Chemical Reagent Co. Ltd. in Tianjin, China.  $\text{NaBH}_4$  and 98%  $\text{CuSO}_4 \cdot 5\text{H}_2\text{O}$  were provided by Yixing Fandao Chemical Factory in Yixing, China. 99.5% D-CA was provided by Sigma. Before use, mutarotation of CA stock solutions was allowed to occur for at least 24 h at 4 °C. Other chemicals were of analytical reagent grade and used as

received. Ultrapure water was provided by a Millipore Milli-Q water purification system, which was used throughout the preparation of all solutions. All electrochemical measurements were performed at ambient temperature ( $25\pm 2$  °C) using a triple-electrode geometry on a CHI 660 electrochemical workstation (Shanghai CH Instrument Co. Ltd., China) and an EC 550 electrochemical workstation (Gaoss Union Technology Co., Ltd., Wuhan, China), with a saturated calomel electrode (SCE), reference electrode and platinum wire counter electrode.

## 2.2. Preparation of nanocomposites

A certain amount of MWCNTs scattered in a  $\text{H}_2\text{SO}_4\text{-HNO}_3$  solution (3:1, v/v) was ultrasonically oscillated for 4 h, after which the MWCNTs were separated through centrifugation. Afterwards, a neutral pH was obtained through adjustment. Quick functional MWCNTs were yielded after repeated washing using acetone, along with drying in a vacuum. Typically, the mixture of 43.6 mg  $\text{KMnO}_4$  and 20 mg MWCNTs was suspended in double-distilled water (24 mL), followed by 0.5 h of sonication. The as-prepared suspension was slowly mixed with ethylene glycol, with magnetic stirring maintained for *ca.* 0.5 h at 50 °C until the  $\text{KMnO}_4$  colour faded, which indicated the complete deposition of  $\text{MnO}_2$  on the MWCNTs. After centrifugation, washing with water, ultra-filtration, and drying for 10 h at 70 °C, the composite products were yielded.

After the dispersion of 25 mg  $\text{MnO}_2\text{-MWCNTs}$  powder into 50 mL water, 0.05 mM  $\text{CuSO}_4\cdot 5\text{H}_2\text{O}$ , 0.1 mM polyethylene glycol (6000), and 0.01 mM ascorbic acid were added, along with 0.1 M NaOH to obtain a neutral pH. Afterwards, reduction with 0.05 M  $\text{NaBH}_4$  was completed. The whole process should be performed under magnetic stirring for 1.5 h. Finally,  $\text{Cu-MnO}_2\text{-MWCNTs}$  nanocomposites in the form of black powder were obtained after washing and centrifugal drying.

## 2.3 Electrochemical measurements

A CHI 660A electrochemical analyser (Shanghai Chenhua Co., China) with a traditional triple-electrode configuration was used for all electrochemical tests. The working, reference, and counter electrodes were a modified glass carbon electrode (GCE; bare GCE,  $\text{MWCNT/GCE}$ ,  $\text{MnO}_2\text{/MWCNT/GCE}$  and  $\text{Cu/MnO}_2\text{/MWCNTs}$ ), a saturated calomel electrode, and a platinum wire. Cyclic voltammetry (CV) was conducted from 0 V to 1 V with a scan rate of 50 mV/s. Current-time (I-T) measurement was conducted at potential of 0.4 to 0.75 V.

## 3. RESULTS AND DISCUSSION

Cyclic voltammetry (CV) measurements were used for the voltammetric characterization of CA. A comparison of the characteristic CVs of CA (5 mM) in  $\text{H}_2\text{SO}_4$  (0.1 M) using a bare GCE, MWCNTs modified GCE and  $\text{MnO}_2\text{-MWCNTs}$  modified GCE is presented in Fig. 1. The bare GCE showed an undesirable defined oxidation peak at 660 mV, which shifted negatively to 541 mV in the case of the MWCNTs modified GCE. Furthermore, the charge transfer processes were highly

reversible, and the real surface area was larger, as evidenced by the increased peak current. In addition, effective improvement of redox current was achieved upon the addition of MnO<sub>2</sub> particles on MWCNTs, suggesting that the presence of MnO<sub>2</sub> particles enhanced the electrode kinetics. The porous structure of the conducting polymer allows dispersion of the metal particles into the polymer matrix and generates additional electrocatalytic sites [35, 36]. The obviously improved current response and subsequent decreased peak potential confirmed the catalysis effect of the MnO<sub>2</sub>-MWCNTs modified GCE in promoting the electrochemical reaction and significantly increasing the charge transfer rate.

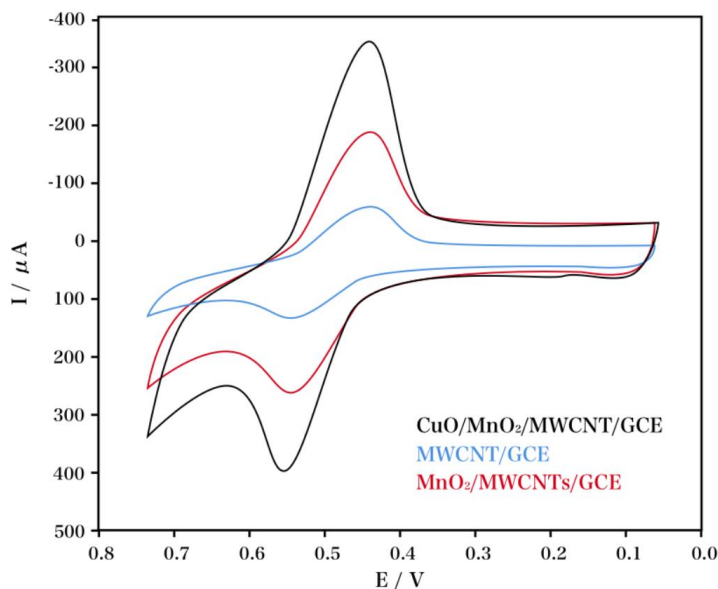


**Figure 1.** CV patterns of CA (5 mM) at a bare GCE, MWCNT modified GCE and MnO<sub>2</sub>-MWCNT modified GCE at a scan rate of 50 mV/s, with the relationship between the square root of the scan rate and anodic peak current shown in the inset.

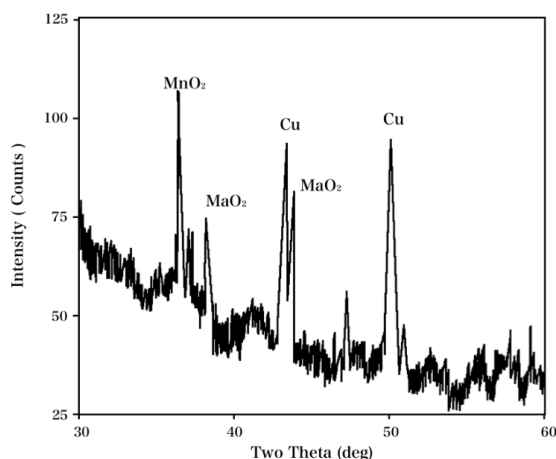


**Figure 2.** XRD profiles of Cu/MnO<sub>2</sub>/MWCNTs nanocomposites.

The Cu/MnO<sub>2</sub>/MWCNTs were characterized via the XRD profiles in Fig. 2, where three main peaks at 50.51° and 43.52° were easily observed through the diffraction pattern. These peaks

corresponded to the diffraction from Cu. Furthermore,  $\text{MnO}_2$  films were formed, as evidenced by several peaks ( $43.8^\circ$ ,  $36.5^\circ$ , and  $38.4^\circ$ ) of  $\text{MnO}_2$  (JCPDS 05-0331). In addition, the attachment of the  $\text{Cu/MnO}_2/\text{MWCNTs}$  film layers to the surface of the electrode was apparent in the XRD characterization.

Both the  $\text{MnO}_2/\text{MWCNTs}/\text{GCE}$  and  $\text{Cu/MnO}_2/\text{MWCNTs}/\text{GCE}$  showed a pair of asymmetric redox peaks in CVs (Fig. 3). The  $\text{Cu/MnO}_2/\text{MWCNTs}/\text{GCE}$  showed much more enhanced peak currents than the  $\text{MnO}_2/\text{MWCNTs}/\text{GCE}$ , corresponding to the promoted  $\text{Cu/MnO}_2$  electrodeposition quantity onto the electrode. Specifically, MWCNTs were exceptional in electrical conductivity, thus increasing the electrodeposition potential. The results also indicated that the  $\text{Cu/MnO}_2/\text{MWCNTs}$  nanocomposite increased the electroactive surface area and that catalytic kinetics is controlled by a diffusion process, which promotes the electron transfer [37].

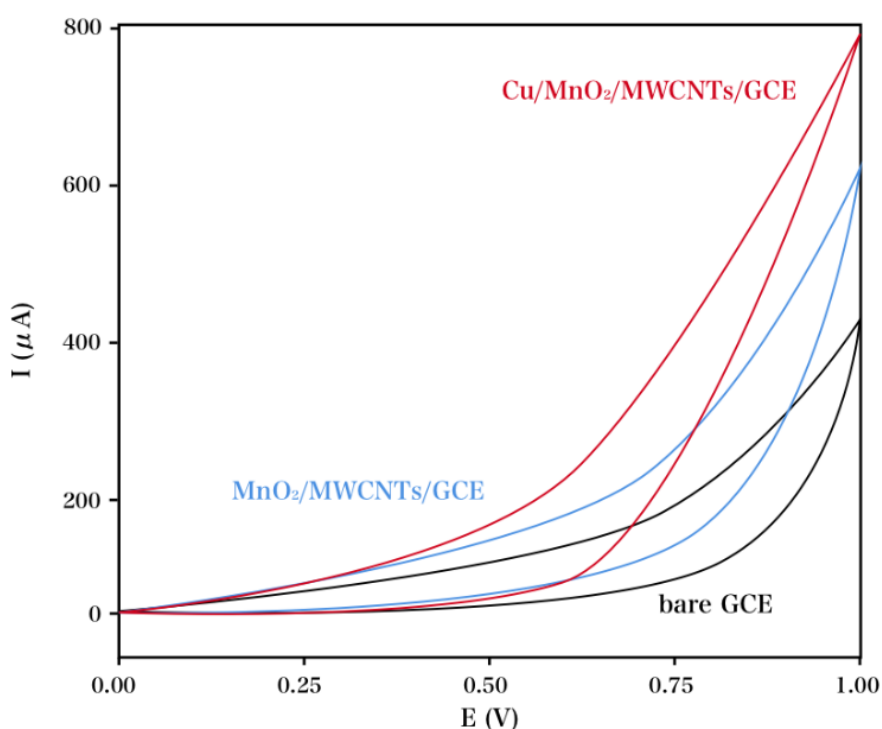


**Figure 3.** CVs of the bare GCE,  $\text{MnO}_2/\text{MWCNTs}/\text{GCE}$  and  $\text{Cu/MnO}_2/\text{MWCNTs}/\text{GCE}$  in 0.50 mM NaOH solution at a scan rate of 50 mV/s.

To enhance the behaviour of our proposed sensor, the effect of the applied potential on the response current of this sensor was studied, as shown in Fig. 4. Varying amperometric response patterns of CA after successively adding CA (1.0 mM) using  $\text{Cu/MnO}_2/\text{MWCNTs}$  nanocomposites were recorded at a potential of 0.4 to 0.75 V. It can be seen that the low working potential results in a very weak CA response due to the insufficient potential for CA electro-oxidation. Enhanced responses can be observed along with an increase in working potential. However, a higher working potential inevitably results in a high background current, which could influence the responses. The maximal response current was obtained when the applied potential was 0.60 V, with the least background noise.

Therefore, the working potential was determined to be 0.60 V in the detection of CA using Cu/MnO<sub>2</sub>/MWCNTs nanocomposites.

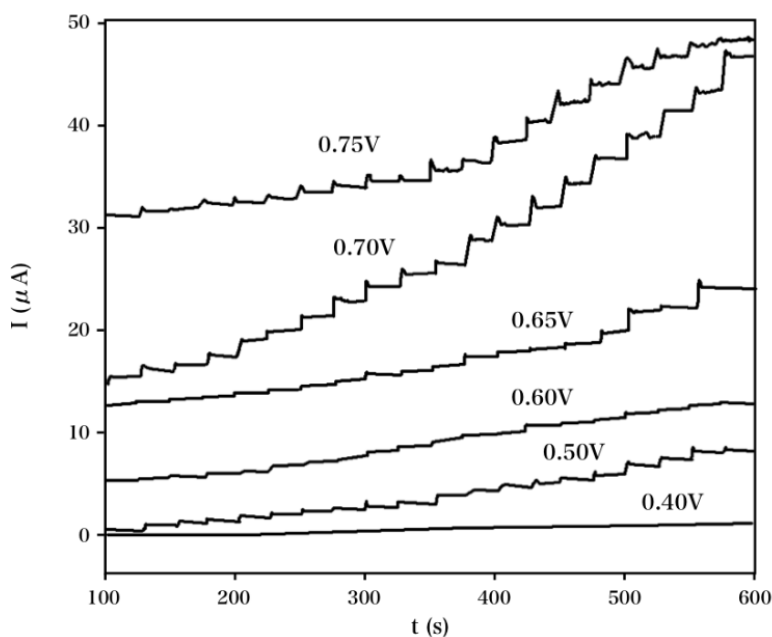


**Figure 4.** Steady-state current–time responses of CA (1.0 mM) in NaOH (50 mM) recorded at different potentials using Cu/MnO<sub>2</sub>/MWCNTs nanocomposites.

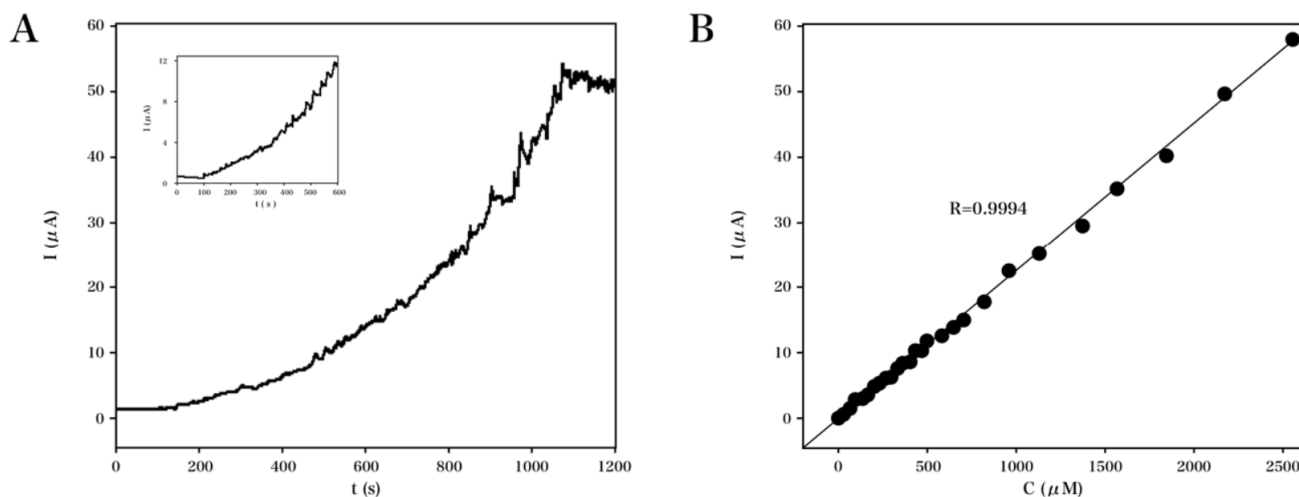


**Figure 5.** (A) Steady-state current–time responses to CA of different concentrations in NaOH (20 mM) at 0.60 V using Cu/MnO<sub>2</sub>/MWCNTs nanocomposites, with the current–time response to CA (0.25 and 2.5 μM) shown in the Inset. (B) Calibration curve vs. the concentration of CA.

Our proposed sensor showed an excellent amperometric response to successive addition of CA with 2 s response time and an LOD of 3 (Fig. 5), with two corresponding calibration curves recorded. The other calibration curve was in a higher concentration range of 0.6 to 2 μM. Our proposed sensor

was highly sensitive, with a wide linear range, low LOD, and short response time. For the oxidation of CA, Cu/MnO<sub>2</sub> on MWCNTs showed an exceptional catalytic effect, as shown below. The electrochemical catalysis of Cu/MnO<sub>2</sub> for the oxidation of CA was reversible and facile, considering the electrochemical redox couple of Cu/MnO<sub>2</sub>/MWCNTs nanocomposites. In addition, during the catalysis process of CA, ample active sites were present due to the morphology of Cu/MnO<sub>2</sub>. Furthermore, the charge transfer between the substrate electrode and Cu/MnO<sub>2</sub> was substantially enhanced by MWCNTs. To allow for comparison with previous reports, the characteristics of different electrochemical sensors for CA are summarized in Table 1.

**Table 1.** Comparison of the major characteristics of electrochemical sensors used for the detection of CA.

Electrode	Linear detection range	Detection limit	Reference
Electrochemically activated CPE	0.5 - 3 $\mu$ M	0.12 $\mu$ M	[38]
Fluorine-doped SnO <sub>2</sub>	2 - 30 $\mu$ M	0.15 $\mu$ M	[39]
Fullerene-CNT/ionic liquid	0.1 - 30 $\mu$ M	0.027 $\mu$ M	[40]
Cu/MnO <sub>2</sub> /MWCNTs	0.6 - 2 $\mu$ M	0.34 $\mu$ M	This work

For our proposed sensor, another significant influencing factor is the interference-free feature. On the Cu/MnO<sub>2</sub>/MWCNT nanocomposites, we studied the electrochemical response of the interference agents (i.e., uric acid (UA), ascorbic acid (AA), dopamine (DA), other carbohydrate compounds, etc.) which are easily oxidative and present in human blood with CA. CA (20  $\mu$ M) and interference agents (10  $\mu$ M) were added into a NaOH solution (50 mM) for the interference analysis, since CA concentrations are at least 30 times greater than those of interference agents in human blood (Fig. 6). The oxidation current sharply increased after adding CA (20  $\mu$ M). However, the current response showed no variation after injecting UA, AA, or DA. The above interference agents could be oxidized under low potential, with insignificant observed signal.

**Table 2.** Determination of serum specimens with our proposed Cu/MnO<sub>2</sub>/MWCNTs sensor and the standard ELISA technique ( $\mu$ M).

Sample	1	2	3	4	5
Cu/MnO <sub>2</sub> /MWCNTs	0.54	0.75	1.02	1.45	1.88
ELISA	0.50	0.73	1.05	1.41	1.90
RSD (%)	4.7	2.2	5.1	3.7	4.2

It can be seen that the electro-catalysis current response was little affected by the interference agents in our case; thus, the Cu/MnO<sub>2</sub>/MWCNTs were selective for the determination of CA. The stability and repeatability of the Cu/MnO<sub>2</sub>/MWCNTs/GCE were evaluated by amperometric measurement in 0.1 M NaOH solution containing 1  $\mu$ M CA. After 5 successive amperometric measurements, no obvious response change was observed, implying that the modified electrode was

very stable. To evaluate the practical application of the proposed sensor, we detected the CA content in the serum samples (Table 2). An ELISA method has been adopted for the purpose of comparison. It can be seen that the proposed Cu/MnO<sub>2</sub>/MWCNTs showed a reliable result for CA determination in a real sample

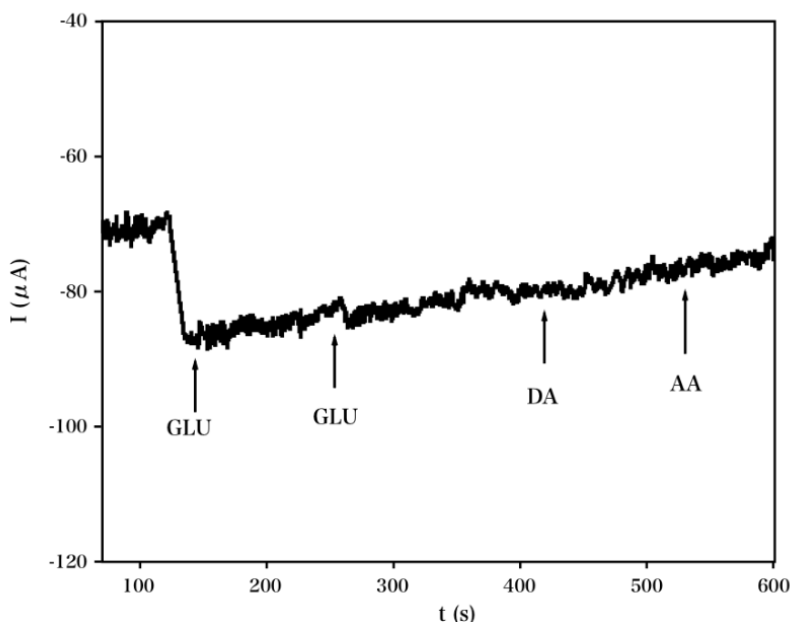


**Figure 6.** The amperometric response of CA (20  $\mu\text{M}$ ), 10  $\mu\text{M}$  ascorbic acid, 10  $\mu\text{M}$  uric acid and 10  $\mu\text{M}$  ascorbic acid. Detection potential: 0.60 V.

#### 4. CONCLUSIONS

This study proposed a Cu/MnO<sub>2</sub>/MWCNT nanocomposite-based sensor for the facile detection of CA. The developed sensor has the potential to be applied to practical circumstances, due to its desirable selectivity, wide linear range, and low LOD. Strong adsorption of MnO<sub>2</sub> could be achieved with the increase in the specific surface area of carboxyl functionalized MWCNTs. The optimal adherence of Cu nanoparticles in the absence of any decomposition was guaranteed and was ascribed to the exceptional uniformity and dispersion of MnO<sub>2</sub>. The dynamic features for the oxidization and catalysis of CA were increased using the new nanocomposites composed of three distinct nanomaterials. Therefore, this study presents a novel strategy for the fabrication of enzymatic sensors suitable for further practical application.

#### References

1. K. Okada, A. Kurita, B. Takase, T. Otsuka, E. Kodani, Y. Kusama, H. Atarashi and K. Mizuno, *International Heart Journal*, 50 (2009) 95.



2. Y. Ruan, L. Zhang, J. Niu and S. Wang, *Wei Sheng Yan Jiu= Journal of Hygiene Research*, 42 (2013) 561.
3. A. Endo, T. Kinugawa, K. Ogino, M. Kato, T. Hamada, S. Osaki, O. Igawa and I. Hisatome, *The American Journal of the Medical Sciences*, 320 (2000) 24.
4. E. Akil, Y. Tamam, M.A. Akil, I. Kaplan, M.Z. Bilik, A. Acar and B. Tamam, *Journal of Neurosciences in Rural Practice*, 6 (2015) 145.
5. A. Barnett, A. Dobson, P. McElduff, V. Salomaa, K. Kuulasmaa and S. Sans, *Journal of Epidemiology & Community Health*, 59 (2005) 551.
6. S. Komulainen, T. Tähtinen, H. Rintamäki, H. Virokannas and S. Keinänen-Kiukaanniemi, *European Journal of Clinical Pharmacology*, 56 (2000) 637.
7. B. Luo, S. Zhang, S. Ma, J. Zhou and B. Wang, *International Journal of Environmental Research and Public Health*, 9 (2012) 2312.
8. J. Ribeiro, P. Fernandes, C. Pereira and F. Silva, *Talanta*, 160 (2016) 653.
9. L. Chen, X. Zhu, J. Shen and W. Zhang, *Analytical and Bioanalytical Chemistry*, 408 (2016) 4987.
10. F. Ghasemi, M.R. Hormozi-Nezhad and M. Mahmoudi, *Analytica Chimica Acta*, 917 (2016) 85.
11. A. Arnold, Y. Tang, K. Qian, L. Shen, V. Valencia, M. Phillips and Y. Zhang, *Journal of Hypertension*, 25 (2007) 197.
12. Z. Zhang, J. Wang, H. Yuan, Y. Gao, D. Liu, L. Song, Y. Xiang, X. Zhao, L. Liu and S. Luo, *The Journal of Physical Chemistry B*, 109 (2005) 18352.
13. M. Fox and R. Wightman, *Pharmacological Reviews*, 69 (2017) 12.
14. E. Wierzbicka and G.D. Sulka, *Sensors and Actuators B: Chemical*, 222 (2016) 270.
15. M. Saraji and A. Shahvar, *Analytical Methods*, 8 (2016) 830.
16. B. Westerink and W. Timmerman, *Analytica Chimica Acta*, 379 (1999) 263.
17. L. Zhang, H. Li, Y. Ni, J. Li, K. Liao and G. Zhao, *Electrochemistry Communications*, 11 (2009) 812.
18. Y. Luo, *Materials Letters*, 61 (2007) 1893.
19. K. Novoselov, A. Geim, S. Morozov, D. Jiang, Y. Zhang, S. Dubonos, I. Grigorieva and A. Firsov, *science*, 306 (2004) 666.
20. C. Batchelor-McAuley, G. Wildgoose, R. Compton, L. Shao and M. Green, *Sensors and Actuators B: Chemical*, 132 (2008) 356.
21. S. Ali, N. Alvi, Z. Ibupoto, O. Nur, M. Willander and B. Danielsson, *Sensors and Actuators B: Chemical*, 152 (2011) 241.
22. C. Zhu, Y. Fang, D. Wen and S. Dong, *Journal of Materials Chemistry*, 21 (2011) 16911.
23. X. Zhang, G. Wang, W. Zhang, Y. Wei and B. Fang, *Biosensors and Bioelectronics*, 24 (2009) 3395.
24. Y. Luo, Y. Tian, A. Zhu, Q. Rui and H. Liu, *Electrochemistry Communications*, 11 (2009) 174.
25. X. Kang, Z. Mai, X. Zou, P. Cai and J. Mo, *Analytical Biochemistry*, 369 (2007) 71.
26. R. Gao and J. Zheng, *Electrochemistry Communications*, 11 (2009) 608.
27. Q. Sheng, K. Luo, J. Zheng and H. Zhang, *Biosensors and bioelectronics*, 24 (2008) 429.
28. R. Prasad and B. Bhat, *Sensors and Actuators B: Chemical*, 220 (2015) 81.
29. R. Sedghi and Z. Pezeshkian, *Sensors and Actuators B: Chemical*, 219 (2015) 119.
30. C. Chen, C. Lin and L. Chen, *Electrochimica Acta*, 152 (2015) 408.
31. A. Zhong, X. Luo, L. Chen, S. Wei, Y. Liang and X. Li, *Microchimica Acta*, 182 (2015) 1197.
32. R. Devasenathipathy, C. Karuppiyah, S. Chen, S. Palanisamy, B. Lou, M. Ali and F. Al-Hemaid, *RSC Advances*, 5 (2015) 26762.
33. X. Du, Z. Miao, D. Zhang, Y. Fang, M. Ma and Q. Chen, *Biosensors and Bioelectronics*, 62 (2014) 73.
34. K. Lin, Y. Lin and S. Chen, *Electrochimica Acta*, 96 (2013) 164.
35. S. Tian, J. Liu, T. Zhu and W. Knoll, *Chemistry of Materials*, 16 (2004) 4103.
36. L. Zhang and M. Wan, *The Journal of Physical Chemistry B*, 107 (2003) 6748.
37. Y. Han, J. Zheng and S. Dong, *Electrochimica Acta*, 90 (2013) 35.

38. S. Chitravathi and N. Munichandraiah, *Journal of The Electrochemical Society*, 162 (2015) B163.
39. C. Ramírez, M. del Valle, M. Isaacs and F. Armijo, *Electrochimica Acta*, 199 (2016) 227.
40. M. Mazloum-Ardakani and A. Khoshroo, *Electrochemistry Communications*, 42 (2014) 9

© 2017 The Authors. Published by ESG ([www.electrochemsci.org](http://www.electrochemsci.org)). This article is an open access article distributed under the terms and conditions of the Creative Commons Attribution license (<http://creativecommons.org/licenses/by/4.0/>).